Design and implement UAV for low-altitude data collection in precision agriculture

Minh-Trung Vu, Truong-Son Nguyen, Cong-Hoang Quach and Minh-Trien Pham

VNU University of Engineering and Technology, 144 Xuan Thuy, Cau Giay, Hanoi, Vietnam

Abstract—**In recent years, along with the development of precision agriculture, Unmanned Aerial Vehicles (UAVs) in crop data collection is becoming more popular because of the advantages of collecting data in a large area. However, many crops and special growing conditions require low-flying UAVs to collect data such as orchards. This challenge with the safety control algorithm of the UAVs. The research aims to develop UAVs capable of autopilot and sampling at low altitudes. The safety control problem of UAV is solved by the Visual Inertial Odometry (VIO) algorithm using a stereo camera synchronized with an inertial measurement unit (IMU). Besides that, the UAV is equipped with a high-resolution RBG camera for data sampling. The system has been tested under various conditions of low-ceiling performance with altitude hold and obstacle avoidance requirements, and the collected data is satisfactory for use.**

Keywords—*UAV, precision agriculture, Visual Inertial Odometry, low-ceiling*

I. INTRODUCTION

In the last few years, the total volume of investments in the agricultural sector has increased by 80%. These investments aim to achieve productivity growth of at least 70% by 2050to meet the advanced needs of 9 billion people. At the same time, the agricultural sector has to address severe challenges such as environmental pollution, the limited availability of arable lands, and the decrease in the number of farmers. Farms must be extended and constantly innovate to improve and maintain productivity to meet the demands. The integration of Unmanned Aerial Vehicles (UAVs) with IoT (Internet of Things) devices, such as embedded sensors and communication elements, for agriculture operations is growing at a significantly faster pace than expected [1], [2]. These IoT devices greatly enhance management operations, including field mapping[3], [4], plant-stress detection [5], [6], biomass estimation [7], [8], weed management [7], [9]inventory counting [10], etc.

UAV's most common application is observing agriculture fields regarding soil conditions, crop growth, weed infestation, insects, plant diseases, and crop water requirements. It provides prescription data to guide the operation of precision implements. Realizing the decisions calls for variable-rate technology to implement tactical actions in seeding, fertilizer/chemical application and irrigation instead of only mapping the field one year for improvements in a subsequent year. Typically, UAVs always using high-range fly combine with high-resolution cameras for the survey mission [11]. However, many crops and special growing conditions require low-flying UAVs to collect data such as orchards. The other type of application is using drones for water crops or pesticide spraying. This application can help reduce herbicide use by 52% in Brazilian soybean field but it cannot work automatically with the auto fly mission in complex farmland at low altitude. In a low-altitude fly range, UAVs will face many risks such as damping GPS, obstacles… Therefore, achieving autonomous recognition of obstacles and real-time avoidance is one of the inevitable trends in the intelligent development of agriculture drone.

Obstacle detection, collision avoidance, path planning, localisation, and control systems are the key parts required by an unmanned vehicle to be fully autonomous and able to navigate without being explicitly controlled [12]. In a challenging dynamic agricultural environment, tasks may become increasingly difficult for UAVs due to on-board payload limitations (e.g., sensors, batteries), power constraints, reduced visibility due to bad weather (e.g., rain, dust), and complications in remote monitoring. The robotics community is striving hard to address these challenges and to bring the technological level suited for the demanding environments ensuring success and safe navigation of the unmanned vehicles[13][14]. Therefor, UAV's controller need a

There has been a lot of research in recent times on visual and visual-inertial odometry for UAVs with a variety of proposed algorithms [15]. A monocular camera is an ideal sensor for this task because of its small size, cheap and straightforward hardware setting. But, there are many problems in the system based on pure vision, so it is difficult to be applied and practice [16]. Besides that, cameras and inertial measurement units have complementary properties. By combining and utilizing their measurement data, robustness and accurate positioning can be well solved. The camera provides rich image information; the data is not easy to drift, contained in the IMU gyroscope, and the accelerometer can accurately provide short-term estimates. Visual and inertial navigation is more and more popular among researchers, especially in UAV[17] .

At present, there are also very excellent visual-inertial navigation research results, such as Hong Kong university of science and technology VINS[18], based on the ORB-SLAM2 improved IMU+ORB-SLAM2 system[19]. There are some problems in the monocular inertial navigation system. Because the monocular camera cannot measure the depth information, the monocular system cannot recover the measurement scale information. Due to the lack of direct distance measurement, the monocular visual structure will be difficult to integrate with the inertial measurement directly. To solve these problems, many systems of stereo-base inertial odometry were proposed [20]. The stereo camera can now obtain the depth information of the object so that the camera data can be better integrated with the IMU data and the system initialization is simpler.

Furthermore, the stereo vision algorithm is excellent to extract information about the relative position of 3D objects and obstacle avoidance in autonomous systems.For example, the article, 3D path-planning and stereo-based obstacle avoidance for rotorcraft demonstrate the complexity of working with the stereo vision to build a 3D occupancy map. The experiments highlighted the need to keep the stereo cameras pointed along the velocity vector to avoid collisions.

In this paper, we design a fully autonomous drone for agriculture, developed and implemented. This design integrated both the stereo camera and an embedded computer for state estimation and obstacle avoidance. This article is divided as follows: Section II inquires on the platform and hardware system for the primary purpose. Section III defines the VIO and obstacle avoidance algorithm. Section IV introduces the results and discussion. Finally, Section V is the conclusion.

,

II. HARDWARE SYSTEM

The specifications for the design were listed in table 1 below, and these determine the choice of the suitable component.

TABLE I.   THE SPECIFICATIONS FOR THE DRONE DESIGN

Parameter	Value
Lifting thrust	10N
Weight	5Kg
Battery	4S 5200mAh
Range of radio frequency coverage	1Km
Frequency of control signals	2.4GHz

A. Hex-copter Body

The frame of the hex-copter was made of very light carbon fiber. Many other materials such as aluminium and wood were considered. But their weight dramatically affects the performance of the aircraft, especially the flight time. The body is divided into three parts: body frame, landing gear, and embedded computer connection path. The body frame enclosed all the needed components. The width of the structure was 450mm, and the height was 400mm.

Before choosing a motor for the design, the total weight needs to estimate first. It was determined by function:

$$Thrust = (weight*2)/6 \ (For \ 2:1 \ thrust \ / \ weight \ ratio \ ) \qquad (1)$$

Where: weight is the estimated weight of the loaded vehicle, which is obtained by adding the individual weights of all components in the aircraft.

B. Embeded computer and camera

Jetson nano was integrated as companion computer because its inherent processing power. It serves as the main control system which changes flight mode via MAVLink protocol. An embedded computer connected to the stereo camera processes images to create depth and visual odometry images to replace GPS data in positioning. Because of the sampling rate and image quality, we use the MyntEye camera.
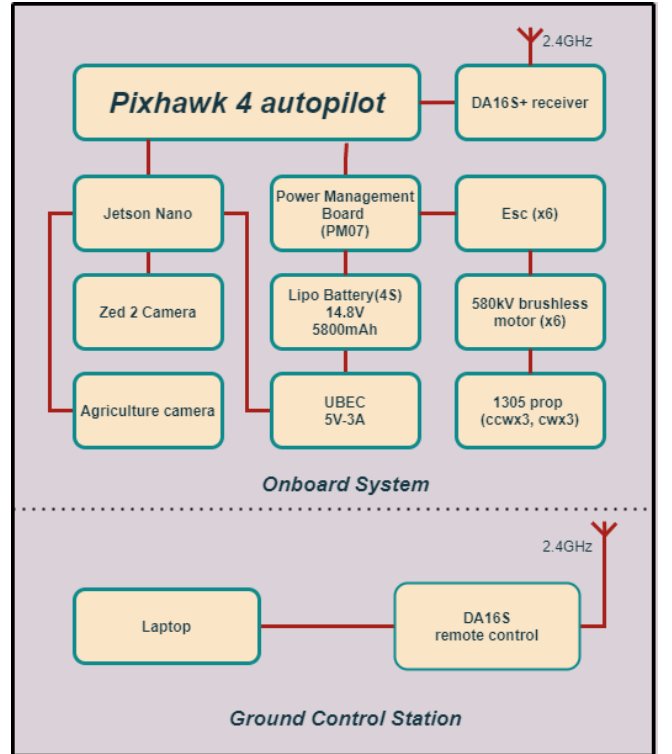
Fig. 1 System connection

III. ALGORITHM

A. Visual-Inertial Odometry

In this paper, we use a VIO system called VINS-Fusion. This is an extended version of VINS-Mono [19]. VINS-Fusion is an optimization-based multi-sensor state estimator, which archives accurate self-localization for autonomous applications (UAVs, cars, AR/VR). It supports multiple visual-inertial sensor types (mono camera with IMU, stereo camera with IMU also only stereo cameras systems). The outstanding advantages of VINS-Fusion are:

- Multiple sensors support
- Online spatial calibration (transform between the camera and IMU)
- Online temporal calibration (time offset between the camera and IMU) [18]

- Visual loop closure

In this system, we use the stereo camera with IMU. The overview of the system is described in Fig. xxx. In the first block, measurement preprocessing, features are extracted and tracked, and IMU measurements between two consecutie stereo frames are preinegrated. The initialization procedure provides all necessary values: pose, velocity, gyroscope bias, and three-dimensional feature location. This information will be used for bootstrapping the subsequent nonlinear optimization based VIO. After successful parameter

initialization, the VIO with relocalization modules will start. This module tightly fuses pre-integrated IMU measurements, feature observations, and redetected feature from the loop closure. Finally, the pose graph module performs global optimization to eliminate drift and achieve reuse propose. Besides, camera-rate pose and IMU-rate pose are used to online temporal calibrate process.
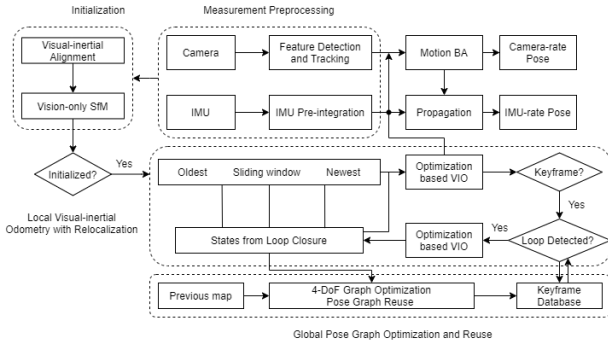
Fig. 2 System overview

B. *Obstacle avoidance algorithm*

Obstacle avoidance is a two-step problem: Obstacle detection and path planning. There exist different algorithms, approaches, and solutions to path planning. The stereo vision camera help to detect an object in front of the drone, and the computer will choose between 4 different flight modes, defined as follows:

- Go to the goal (GTG): Only used when no obstacle is detected. The quadcopter goes in a straight line toward its intended destination (waypoint to waypoint).
- Avoid obstacle (AO): This is safe mode. Suppose the block gets too close to the drone. It will fly in the opposite direction of the aiming vector from the center of the UAV to the nearest sensed point.
- Avoid obstacle and go-to-goal (AO+GTG): This mode is used when an avoidable obstacle is sensed. It uses the result of a weighted sum vector between GTG and AO to decide where the flight direction will be.
- Follow wall (FW): Special mode in which the perceived obstacle is between the UAV and its target and the GTG + AO mode is not enough to evade said obstacle. The UAV follows the estimated contour of the obstacle until it is circumvented and then switches mode depending on the information available.

Algorithm 1 shows how a mode is chosen considering the available information and vectors. The transitions between modes are illustrated in the Finite State machine displayed in Fig3. Furthermore, the vectors mentioned in the description are represented in Fig4.

The algorithm is defined by information obtained from stereo vision. The closest distance measured by depth image was generated from the stereo camera. It is from smallest to highest and the angles at which each of the length were measured. Once a flight mode is chosen, the companion computer will send a flight control command to the flight controller with velocity vector format.
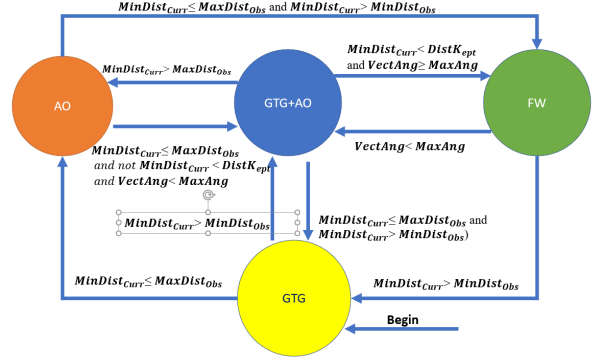
.
Fig. 3 Mode transitions specified in Algorithm 1 represented by a Finite State Machine. The algorithm begins in the GTG mode and should end in the same mode.
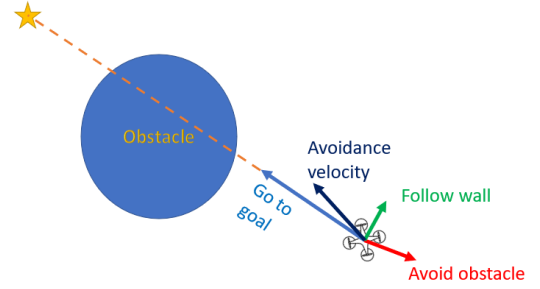
Fig. 4 Vectors used in the obstacle avoidance algorithm to choose the current mode and flight trajectory

---

Algorithm 1 Decision Making

Input: Current Mode CM, Go To Goal Vector $GTGV_{etc}$, Avoid Obstacle Vector AOV_{etc}, Current Minimum Distance to Closest Detected Obstacle $MinDist_{Curr}$

Output: Current Mode CM

Initialization :

1: Define maximum perceivable distance to obstacle$MaxDist_{Obs}$

2: Define minimum permissible distance to obstacle $MinDist_{Obs}$

3: Define distance to keep from estimated wall $DistK_{ept}$

4: Define maximum angle admissible between $GTBV_{ect}$ and AOV_{ect}, $MaxAng$

Main Loop :

5: $VectAng \leftarrow$ angleBetweenVectors($GTBV_{ect}$, AOV_{ect})

6: if ($CM = GTG$) **then**

7: **if** ($MinDist_{Curr} \leq MaxDist_{Obs}$ and $MinDist_{Curr} > MinDist_{Obs}$) **then**

```
8:           CM ← GTG+AO
9:      else if (MinDist_Curr ≤ MinDist_Obs) then
10:          CM ← AO
11:     end if
12: else if (CM = GTG+AO) then
13:     if (MinDist_Curr > MaxDist_Obs) then
14:          CM ← GTG
15:     else if (MinDist_Curr ≤ MinDist_Obs) then
16:          CM ← AO
17:     else if (MinDist_Curr < DistK_ept
and VectAng ≥ MaxAng) then
18:          CM ← FW
19:     end if
20: else if (CM = AO) then
21:     if (MinDist_Curr > MinDist_Obs) then
22:         if (MinDist_Curr < DistK_ept
and VectAng ≥ MaxAng) then
23:              CM ← FW
24:         else
25:              CM ← GTG+AO
26:         end if
27:     end if
28: else if (CM = FW) then
29:     if (VectAng < MaxAng) then
30:          CM ← GTG+AO
31:     else if (MinDist_Curr > MaxDist_Obs) then
32:          CM ← GTG
33:     end if
34: end if
```


Figure 1. Environment simulation

Firstly, for the VO/VIO algorithms our experimental simulated a quadcopter with front stereo camera with: 720x480 resolution and 90° FOV. Simulation environment was built on UE4 software and drone, camera was setting by Airsim open-source. This is a grass field with tree and rock (Figure.1). For the pre-processing, we calibrate the camera first to find project matrix for the VIO algorithm input. And the result of VIO was show below:
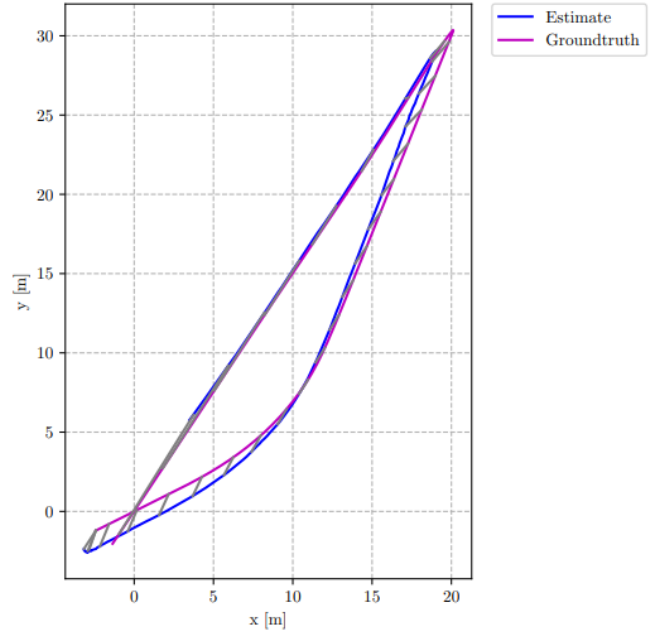
Figure 2.Trajectory simulation

IV. EXPERIMENTS AND RESULT

In this section, we present our experiments with the system. The first part is to evaluate VINS-Fusion with the VIODE dataset [21], then to verify the obstacle avoidance algorithm. All these experiments were conducted in the AirSim simulation environment.

VIODE (VIO dataset in Dynamic Environments) is a benchmark for assessing the performance of VO/VIO algorithms in dynamic scenes. The environments are simulated using AirSim [ref], a photorealistic simulator geared towards developing perception and control algorithms. VIODE's unique advantage over existing datasets lies in the systematic introduction of dynamic objects in increasing numbers and different environments. VIODE uses the same UAV trajectory to generate data series with growing moving objects in each scenario. Thus, with VIODE, we can isolate the influence of scene dynamics on the robustness of vision-based localization algorithms.

Figure 3. Translation error and Yaw error depend on distance

Figure.2 show the trajectory of drone in simulation with velocity 5m/s. In the first straight travelling, the translation error is insignificant (Figure.3). During the next move, the system error was too big due to the drone's rotation and environment didn't enough marker.

Because of the errors in the VIO algorithm, applying the obstacle avoidance algorithm, we reduced the flight speed to 2m/s and got the results as shown in the figure 4.
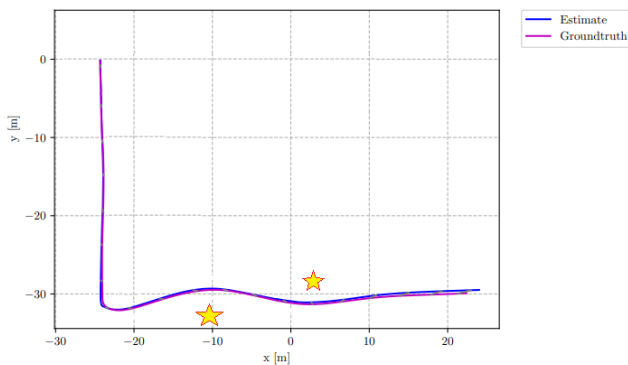
Figure 4. Trajectory in Obstacle avoidance

To investigate how the speed affects the algorithm, we tested the system many times with the camera sampling rate of 25 fps and the 50m distance results are shown below.

Velocity	Translation error
5 m/s	7,4%
4 m/s	5,2%
3 m/s	3,6%
2 m/s	1,4%

V. CONCLUSION

In conclusion, this device could potentially detect and avoid most obstacles. But only using a front stereo camera is used in this implement; obstacles below, behind and above drones may not be possible. Therefore, the drone cannot run in a more complex scenario and at high speed in the current state. Regardless, more tests will be undertaken to assess the current system's limitations and identify possible avenues for improvement. Furthermore, since most of the exposed behaviors rely on practical insights and geometrical calculations, a thorough mathematical proof of the algorithm has not been developed; therefore, future work will focus on deriving it. The VIO system error is insignificant, so it can replace GPS, but after a long time run, the cumulative error needs to be correct. In the future, we will improve the solution as well as the accumulated error.

…

…

[1]   D. C. Tsouros, S. Bibi, and P. G. Sarigiannidis, "A review on UAV-based applications for precision agriculture," *Inf.*, vol. 10, no. 11, 2019, doi: 10.3390/info10110349.

[2]   U. R. Mogili and B. B. V. L. Deepak, "Review on Application of Drone Systems in Precision Agriculture," *Procedia Comput. Sci.*, vol. 133, pp. 502–509, 2018, doi: 10.1016/j.procs.2018.07.063.

[3]   S. Marino and A. Alvino, "Detection of Spatial and Temporal Variability of Vegetation Indices," *Agronomy*, vol. 9, no. 226, p. 13, 2019.

[4]   P. Surový, N. Almeida Ribeiro, and D. Panagiotidis, "Estimation of positions and heights from UAV-sensed imagery in tree plantations in agrosilvopastoral systems," *Int. J. Remote Sens.*, vol. 39, no. 14, pp. 4786–4800, 2018, doi: 10.1080/01431161.2018.1434329.

[5]   C. Cilia *et al.*, "Nitrogen status assessment for variable rate fertilization in maize through hyperspectral imagery," *Remote Sens.*, vol. 6, no. 7, pp. 6549–6565, 2014, doi: 10.3390/rs6076549.

[6]   M. Zaman-Allah *et al.*, "Unmanned aerial platform-based multi-spectral imaging for field phenotyping of maize," *Plant Methods*, vol. 11, no. 1, pp. 1–10, 2015, doi: 10.1186/s13007-015-0078-2.

[7]   A. Chang, J. Jung, M. M. Maeda, and J. Landivar, "Crop height monitoring with digital imagery from Unmanned Aerial System (UAS)," *Comput. Electron. Agric.*, vol. 141, pp. 232–237, 2017, doi: 10.1016/j.compag.2017.07.008.

[8]   E. Honkavaara *et al.*, "HYPERSPECTRAL REFLECTANCE SIGNATURES and POINT CLOUDS for PRECISION AGRICULTURE by LIGHT WEIGHT UAV IMAGING SYSTEM," *ISPRS Ann. Photogramm. Remote Sens. Spat. Inf. Sci.*, vol. 1, no. September, pp. 353–358, 2012, doi: 10.5194/isprsannals-I-7-353-2012.

[9]   M. Pflanz, H. Nordmeyer, and M. Schirrmann, "Weed mapping with UAS imagery and a bag of visualwords based image classifier," *Remote Sens.*, vol. 10, no. 10, pp. 1–17, 2018, doi: 10.3390/rs10101530.

[10]   M. Rahnemoonfar and C. Sheppard, "Deep count: Fruit counting based on deep simulated learning," *Sensors (Switzerland)*, vol. 17, no. 4, pp. 1–12,

2017, doi: 10.3390/s17040905.

[11] Y. Huang, S. J. Thomson, H. J. Brand, and K. N. Reddy, "Development and evaluation of low-altitude remote sensing systems for crop production management," *Int. J. Agric. Biol. Eng.*, vol. 9, no. 4, pp. 1–11, 2016, doi: 10.3965/j.ijabe.20160904.2010.

[12] A. Foka, "Real-Time Hierarchical POMDPs for Autonomous Robot Navigation 2 Partially Observable Markov Decision Processes (POMDPs)," no. July, 2005.

[13] J. N. Yasin, S. A. S. Mohamed, M. H. Haghbayan, J. Heikkonen, H. Tenhunen, and J. Plosila, "Unmanned Aerial Vehicles (UAVs): Collision Avoidance Systems and Approaches," *IEEE Access*, vol. 8, pp. 105139–105155, 2020, doi: 10.1109/ACCESS.2020.3000064.

[14] S. S. Esfahlani, "Mixed reality and remote sensing application of unmanned aerial vehicle in fire and smoke detection," *J. Ind. Inf. Integr.*, vol. 15, no. June 2018, pp. 42–49, 2019, doi: 10.1016/j.jii.2019.04.006.

[15] R. Munguía, S. Urzua, Y. Bolea, and A. Grau, "Vision-based SLAM system for unmanned aerial vehicles," *Sensors (Switzerland)*, vol. 16, no. 3, pp. 1–23, 2016, doi: 10.3390/s16030372.

[16] Y. Li and S. B. Lang, "A Stereo-Based Visual-Inertial Odometry for SLAM," *Proc. - 2019 Chinese Autom. Congr. CAC 2019*, pp. 594–598, 2019, doi: 10.1109/CAC48633.2019.8997432.

[17] D. Scaramuzza and Z. Zhang, "Odometry of," pp. 1–9, 2020.

[18] T. Qin and S. Shen, "[Best Student Paper Award] Online Temporal Calibration for Monocular Visual-Inertial Systems," *Iros*, pp. 3662–3669, 2018, [Online]. Available: http://arxiv.org/abs/1808.00692.

[19] T. Qin, P. Li, and S. Shen, "VINS-Mono: A Robust and Versatile Monocular Visual-Inertial State Estimator," *IEEE Trans. Robot.*, vol. 34, no. 4, pp. 1004–1020, 2018, doi: 10.1109/TRO.2018.2853729.

[20] C. Chen, H. Zhu, M. Li, and S. You, "A review of visual-inertial simultaneous localization and mapping from filtering-based and optimization-based perspectives," *Robotics*, vol. 7, no. 3, 2018, doi: 10.3390/robotics7030045.

[21] K. Minoda, F. Schilling, V. Wuest, D. Floreano, and T. Yairi, "VIODE: A Simulated Dataset to Address the Challenges of Visual-Inertial Odometry in Dynamic Environments," *IEEE Robot. Autom. Lett.*, vol. 6, no. 2, pp. 1343–1350, 2021, doi: 10.1109/LRA.2021.3058073.